Supplemental Material: A polaron-polariton light-emitting diode

Yuanjun Guan[1†], Mengyao Xu[1†], Zhen Cui[2,3†], Xingzhou Chen[1], Chengye Ding[1], Xiaoqing Zhou[2,3], Kenji Watanabe[4], Takashi Taniguchi[5], Jesper Levinsen[6], Meera M. Parish[6], Pavlos G. Savvidis[2,3], Zhe-Yu Shi[1*], Zheng Sun[1,8*], Jian Wu[1,7,9*]

[1]State Key Laboratory of Precision Spectroscopy, East China Normal University, Shanghai, 200241, China.
[2]Department of Physics, School of Science, Westlake University, Hangzhou, Zhejiang, 310024, China.
[3]Institute of Natural Sciences, Westlake Institute for Advanced Study, Hangzhou, Zhejiang, 310024, China.
[4]Research Center for Electronic and Optical Materials, National Institute for Materials Science, Tsukuba, Ibaraki, 305-0044, Japan.
[5]Research Center for Materials Nanoarchitectonics, National Institute for Materials Science, Tsukuba, Ibaraki, 305-0044, Japan.
[6]School of Physics and Astronomy, Monash University, Victoria, 3800, Australia.
[7]Collaborative Innovation Center of Extreme Optics, Shanxi University, Taiyuan, Shanxi, 030006, China.
[8]Shanghai Key Laboratory of Magnetic Resonance, School of Physics and Electronic Science, East China Normal University, Shanghai, 200241, China.
[9]Chongqing Key Laboratory of Precision Optics, Chongqing Institute of East China Normal University, Chongqing, 401121, China.

*Corresponding author(s). E-mail(s): zyshi@lps.ecnu.edu.cn; zsun@lps.ecnu.edu.cn; jwu@phy.ecnu.edu.cn;
†These authors contributed equally to this work.

S1 Angle-resolved reflectivity and PL spectra under the application of a negative external voltage

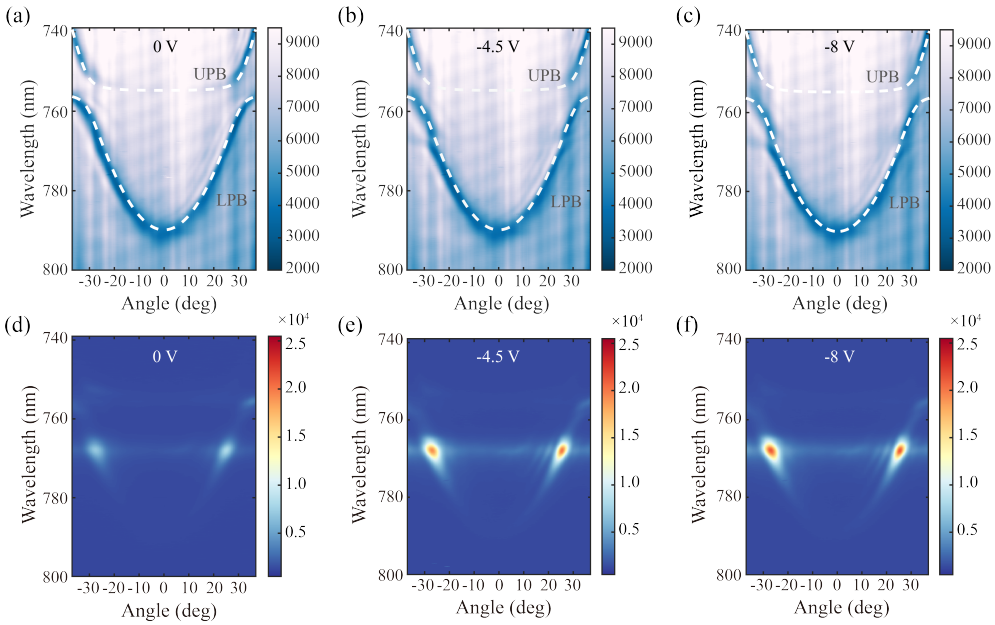

Fig. S1 Angle-resolved reflectivity and PL spectra in the hole-doped regime ($V_{\text{gate}} < 0$). (a)-(c) Angle-resolved reflectivity spectra across varying gate voltages, where hole density correlates directly with the applied gate voltage. The absence of gap formation near the resonance between trion and exciton energies, even at highly negative gate voltages, indicates that these spectral characteristics align more closely with the traditional exciton-polariton framework rather than the electron-doped regime's polaron-polariton model discussed in the main text. The dashed curves are calculated based on the exciton-polariton assumption. (d)-(f) The corresponding angle-resolved PL spectra.

S2 Doping-dependent evolution of E_A, E_R and Z_A, Z_R in the negative voltage regime

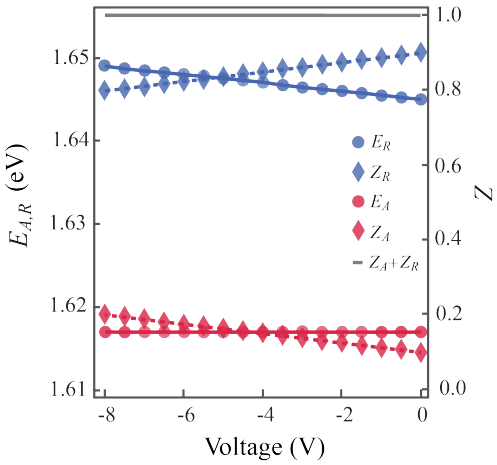

Fig. S2 The extracted energies and quasiparticle residues as a function of the gate voltage in the hole-doped regime. Our methodology involves extracting data through polaron-polariton assumptions and applying the three-oscillator model outlined in the main text. The quasiparticle residues demonstrate consistent values of $Z_A \approx 0$ and $Z_R \approx 1$ throughout the regime, presenting a distinct contrast to the results shown in Fig. 3(f) of the main text. The energy differential follows the relationship $E_R - E_A \approx \epsilon_T - k \cdot V_{\text{gate}}$ with $k = 0.3\,\text{meV} \cdot \text{V}^{-1}$, indicating a very small Fermi energy of $E_F \lesssim 1.6\,\text{meV} \approx 2k_BT$ across the entire range of the gate voltage. This finding confirms the absence of a Fermi sea in the hole-doped regime, suggesting the system should be viewed as conventional exciton-polaritons. This characteristic additionally accounts for the absence of a second gap in the high-voltage regime reflectivity spectra shown in Fig. S1. The observed asymmetry between positive and negative gate voltage regimes can be attributed to the differential Schottky barriers present in electron and hole doping, a characteristic feature of gate-induced doping processes.

S3 Angle-resolved electroluminescence spectra under the application of a negative external voltage

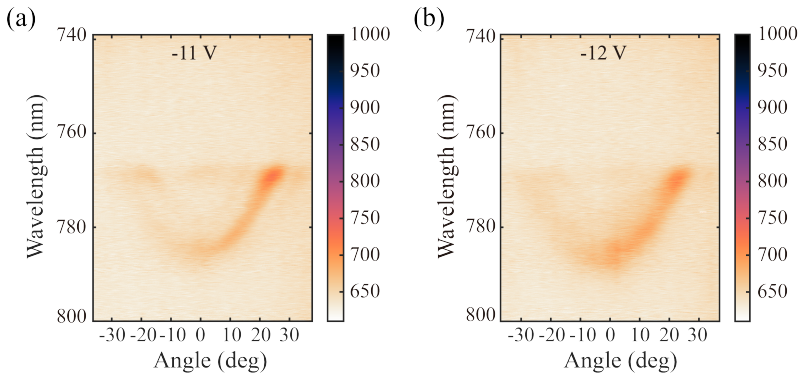

Fig. S3 Angle-resolved electroluminescence (EL) spectra at negative voltages of −11 V (left) and −12 V (right), respectively.

S4 The calculation of reflectivity and PL spectra using the three-oscillator model

Following ref. [1], the reflectivity spectrum of the three-oscillator model is related to the cavity spectral density $A_c(k_\parallel, \omega)$, which is given by

$$A_c(k_\parallel, \omega) = -\frac{1}{\pi}\eta_c^{\mathrm{T}}\left[\omega - H(k_\parallel)\right]^{-1}\eta_c, \tag{1}$$

where $\eta_c = (1, 0, 0)^{\mathrm{T}}$ is the state vector of the cavity mode.

To convert the spectral density $A(k_\parallel, \omega)$ into the reflectivity spectrum $R(\theta, \lambda)$ in the (angle, wave length) space, we utilize the relation $k_\parallel = (\omega/c) \times (\sin\theta)$ and $\omega = 2\pi c/\lambda$. This gives the explicit relation for the reflectivity spectrum,

$$R(\theta, \lambda) = \left|\frac{\partial(k_\parallel, \omega)}{\partial(\theta, \lambda)}\right| A_c(k_\parallel, \omega), \tag{2}$$

where $\frac{\partial(k_\parallel, \omega)}{\partial(\theta, \lambda)}$ stands for the Jacobian determinant.

The detailed balance relation [1–9] indicates the PL spectrum $P(\theta, \lambda)$ is related to the exciton spectral density by

$$P(\theta, \lambda) = e^{-\frac{\hbar\omega}{k_{\mathrm{B}}T_{\mathrm{eff}}}}\left|\frac{\partial(k_\parallel, \omega)}{\partial(\theta, \lambda)}\right| A_X(k_\parallel, \omega). \tag{3}$$

Here, $A_X(k_\parallel, \omega)$ is the exciton spectral density, which is given by

$$A_X(k_\parallel, \omega) = -\frac{1}{\pi}\left\{Z_A\eta_A^{\mathrm{T}}\left[\omega - H(k_\parallel)\right]^{-1}\eta_A + Z_R\eta_R^{\mathrm{T}}\left[\omega - H(k_\parallel)\right]^{-1}\eta_R\right\}, \tag{4}$$

where $\eta_A = (0, 1, 0)^{\mathrm{T}}$, $\eta_R = (0, 0, 1)^{\mathrm{T}}$ are the state vectors of the AP and RP, respectively. It is worth noting that the relation in eq. (3) has been independently discovered multiple times in various contexts. For a brief overview of the historical development, please refer to Ref. [1].

The parameter T_{eff} represents the effective temperature of the doped carrier, which according to our fitting is around 170 K across the entire doping regime. Note that the effective temperature is significantly higher than the lattice temperature, which is around 10 K. We believe that the discrepancy comes from the heat introduced by the optical pump combined with the low efficiency of thermal conduction. Furthermore, one can also see that the Boltzmann factor $e^{-\frac{\hbar\omega}{k_{\mathrm{B}}T_{\mathrm{eff}}}}$ in front of the RHS naturally reduces the intensity of the higher energy parts of the PL spectra, which can be observed in Fig. S1(d,e,f) and Fig. 2(c,d) of the main text.

S5 The calculation of external quantum efficiency η_{EQE}

The external quantum efficiency (EQE) is defined as the ratio of the number of photons emitted by the device to the number of carriers injected, which is related to the tunneling current i through

$$\eta_{\mathrm{EQE}} = \frac{N_{\mathrm{photon}}}{N_{\mathrm{carrier}}} = \frac{N_{\mathrm{photon}}}{i/e}. \tag{5}$$

Here, N_{photon} denotes the number of photons emitted from the device per second, while N_{carrier} refers to the number of injected doping carriers per second. We made adjustments to account for the number of photons detected by the spectrometer, factoring in the system's collection efficiency α and the proportion of the collection angle relative to the total solid angle [10],

$$N_{\mathrm{photon}} = N_{\mathrm{detected}} \times \alpha \times \beta. \tag{6}$$

Here, N_{detected} refers to the intensity measured by the spectrometer. Since the numerical aperture (N.A.) of the collection objective is 0.6, only a fraction of the spontaneously emitted light is captured. Consequently, the solid angle collection efficiency is expressed as $\beta = 1 - \frac{\sqrt{3}}{2}$. To determine N_{photon}, it is necessary to measure α under the same conditions used for previous measurements. We use a 780 nm laser for system calibration, as its photon energy E is approximately equivalent to that of the emitted light from the sample. The optical path for both laser incidence and emission is identical to that used in prior tests, and all spectrometer settings remain unchanged. The laser power P is measured using a power meter,

$$\alpha = \frac{N_{\mathrm{laser}} \times E}{P}, \tag{7}$$

where N_{laser} is laser photon counts per second.

Combining the above formulae, we eventually obtain the external quantum efficiency is

$$\eta_{\mathrm{EQE}} = \frac{N_{\mathrm{photon}} \times P}{N_{\mathrm{laser}} \times E}. \tag{8}$$

References

[1] Tiene, A., Mulkerin, B.C., Levinsen, J., Parish, M.M., Marchetti, F.M.: Crossover from exciton polarons to trions in doped two-dimensional semiconductors at finite temperature. Physical Review B **108**, 125406 (2023)

[2] Kubo, R.: Statistical-mechanical theory of irreversible processes. i. general theory and simple applications to magnetic and conduction problems. Journal of the physical society of Japan **12**(6), 570–586 (1957)

[3] Martin, P.C., Schwinger, J.: Theory of many-particle systems. i. Physical Review **115**(6), 1342 (1959)

[4] Kennard, E.: On the thermodynamics of fluorescence. Physical Review **11**(1), 29 (1918)

[5] Stepanov, B.I.: Universal relation between the absorption spectra and luminescence spectra of complex molecules. In: Doklady Akademii Nauk, vol. 112, pp. 839–841 (1957). Russian Academy of Sciences

[6] McCumber, D.: Einstein relations connecting broadband emission and absorption spectra. Physical Review **136**(4A), 954 (1964)

[7] Van Roosbroeck, W., Shockley, W.: Photon-radiative recombination of electrons and holes in germanium. Physical Review **94**(6), 1558 (1954)

[8] Liu, W.E., Shi, Z.-Y., Parish, M.M., Levinsen, J.: Theory of radio-frequency spectroscopy of impurities in quantum gases. Physical Review A **102**(2), 023304 (2020)

[9] Liu, W.E., Shi, Z.-Y., Levinsen, J., Parish, M.M.: Radio-frequency response and contact of impurities in a quantum gas. Physical Review Letters **125**(6), 065301 (2020)

[10] Gu, J., Chakraborty, B., Khatoniar, M., Menon, V.M.: A room-temperature polariton light-emitting diode based on monolayer WS_2. Nature Nanotechnology **14**(11), 1024–1028 (2019)